16 Apr 2004, 1:30pm - 3:30pm

Effects of Liquefaction on the Numerical Analysis of a Single Pile-Soil Interaction During Earthquakes

Fusao Oka
Kyoto University, Kyoto, Japan

Lu Chih-Wei
Former student of Kyoto University

Zhang Feng
Gifu University, Gifu, Japan

Proceedings: Fifth International Conference on Case Histories in Geotechnical Engineering
New York, NY, April 13-17, 2004

EFFECTS OF LIQUEFACTION ON THE NUMERICAL ANALYSIS OF A SINGLE PILE-SOIL INTERACTION DURING EARTHQUAKES

Fusao Oka
Kyoto University
Kyoto 606-8501 Japan

Lu Chih-Wei
Former student
of Kyoto University

Zhang Feng
Gifu University
Gifu Japan

ABSTRACT

Dynamic behavior of pile-foundations during earthquakes is important for the performance of many foundations. To clarify the mechanism of the soil-pile interaction, we have conducted a series of numerical analysis of a single pile foundation in the different types of a two-layer ground. Upper layer of the ground is composed of dense sand, reclaimed soils, medium dense sand or loose sand, and the lower layer of the ground is composed of clayey soils. In the liquefaction analysis, we have used a fully coupled effective stress analysis method with the cyclic elasto-plastic and elasto-viscoplastic constitutive models for sandy soils and clays. In the FEM, u-p(solid phase displacement-pore water pressure) formulation is adopted. From the numerical results, effect of liquefaction on the single pile-soil interaction has been clarified.

INTRODUCTION

Many structures were damaged during the 1995 Hyogoken-Nambu Earthquake. It was found from the field investigations after the earthquake that not only the pile heads, but also the lower parts of the piles had cracked or failed. This phenomenon indicates that both the inertia force from the upper structure and the kinematic interaction between the piles and the ground play important roles in the mechanical behavior of piles. In particular, when the ground surrounding a structure liquefies due to seismic excitations, the behavior of the piles is more complicated. Damage related to liquefaction may involve cases in which the pile foundation is damaged due to the lateral flow of liquefied soils, and/or the piles fail at the boundary between two different soil layers, of which one liquefies while the other does not. In this study, we conducted a series of numerical simulations to study the dynamic behavior of a single-pile foundation constructed in a two-layer ground, whose upper layer is filled with sandy soils which are dense sand, reclaimed soils, medium dense sand or loose sand, respectively and the lower layer is filled with clayey soils employing a three dimensional liquefaction analysis method (LIQCA3D) to clarify the mechanism of the interactions among the soil-pile-structure.

MODELS FOR SOILS AND PILES

The two-layer ground is typical at near shore of the major Japanese urban cities such as Kobe. In order to study the influence of soil characteristics, four different sandy materials are considered for upper sandy ground, that is, dense sand, medium dense sand, loose sand, and reclaimed soil. Table 1 shows the constitutive parameters in the soil constitutive models for different soils. On the other hand, an axial force dependent (AFD) model (Zhang et al., 2002) is used to describe the dynamic behavior of the pile which is 1.5 m in diameter. The parameters are shown in Table 2.

In the finite element analysis, a cyclic elasto-plastic model is used for sandy soils which has been developed by Oka et al. (1999). The model has been formulated based on: 1. infinitesimal strain theory, 2.elasto-plastic theory, 3.non-associated flow rule, 4.overconsolidated boundary surface, 5. non-linear kinematical hardening rule. The flow rule is a generalized one as:

$$d\varepsilon_{ij}^{p} = H_{ijkl}\frac{\partial f_p}{\partial \sigma'_{kl}} \tag{1}$$

where $d\varepsilon_{ij}^{p}$ is an plastic strain increment tensor, f_p is a plastic potential function and H_{ijkl} is a fourth order isotropic tensor of hardening modulus.

In the model, two yield surfaces are used: one is for the change of stress ratio and the other is for the change of mean effective stress. The yield surface for the change of stress ratio is as:

$$f_y = \{(\eta_{ij}^{*} - x_{ij}^{*})(\eta_{ij}^{*} - x_{ij}^{*})\}^{1/2} - k = 0 \tag{2}$$

$$\eta_{ij}^{*} = s_{ij}/\sigma'_{m}$$

where S_{ij} is the deviatoric stress tensor and σ'_m is the mean effective stress, and x_{ij} is a kinematic hardening parameter whose evolutional law is given by

in the pile segment at the boundary between soil layers.

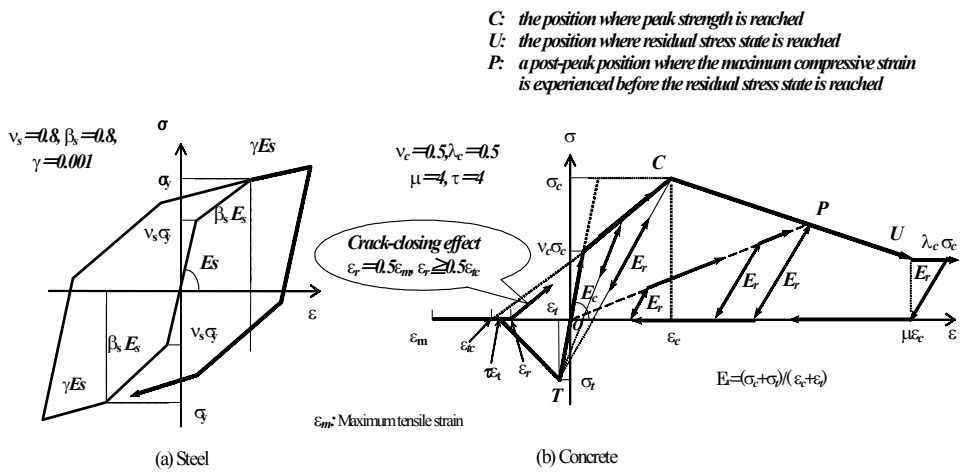

Fig. 1. Stress-strain relations of steel and concrete

$$dx_{ij} = B^*(A^* de_{ij}^p - x_{ij}^* d\gamma^{p^*}) \quad (3)$$

$$d\gamma_p = (de_{ij}^p de_{ij}^p)^{1/2}$$

where de_{ij}^p is the plastic deviatoric strain increment, A* and B* are material constants.

For clay layer of base ground, an elasto-viscoplastic model (Oka, 1992)was used.

NUMERICAL SIMULATION METHODS

The governing equations for the coupling problems between soil skeleton and pore water pressure are obtained based on the two-phase mixture theory (Biot, 1962). Using a u-p (displacement of the solid phase-pore water pressure) formulation (Zienkiewicz, 1982), the liquefaction analysis is formulated. The side boundaries of the simulated system are assumed to be equal-displacement boundaries, the bottom of the system is fixed and boundaries except surface of the ground are impermeable. In this dynamic analysis, a stiffness-matrix-dependent type of Rayleigh damping is adopted and the direct integration method of Newmark-β is used in this dynamic analysis with a time interval 0.01 sec. Ground water table is at 1.5m beneath the ground surface. The mass of the superstructure is 80,000 Kg and the height of pier is 8m. Figure 1 shows the configuration of the single pile system and the seismic wave used in this study.

RESULTS AND DISCUSSIONS

Figure 5 shows the history of effective stress decrease ratio (ESDR) of soil in the middle of different type of sandy layers. Liquefaction occurs when ESDR equals to 1. It can be seen that loose sand easily liquefies entirely and medium sand and reclaimed soil almost liquefy at the end of the major seismic event (t=10sec), while the effective stress of dense sand does not decrease much at all. Figure 6 shows the histories of bending moment at pile head and

Since dense sand layer does not liquefy at all, the earthquake wave motion does not deamplify and the largest bending moment occurs at the pile head among the cases. On the other hand, the larger bending moments occur in the pile at the boundary between layers at t=4sec and t=7sec for loose sand, and medium dense sand and reclaimed soils, respectively, when the effective stress of the sand layers decreases significantly.

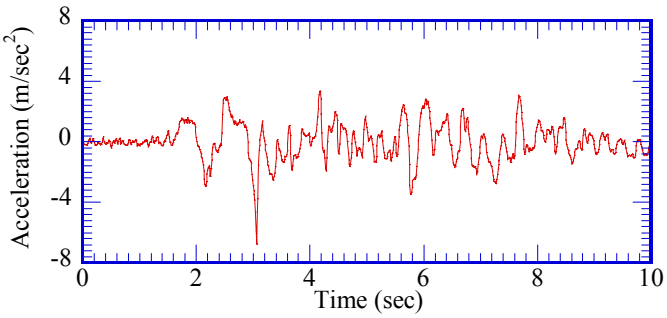

Fig.2. Input wave

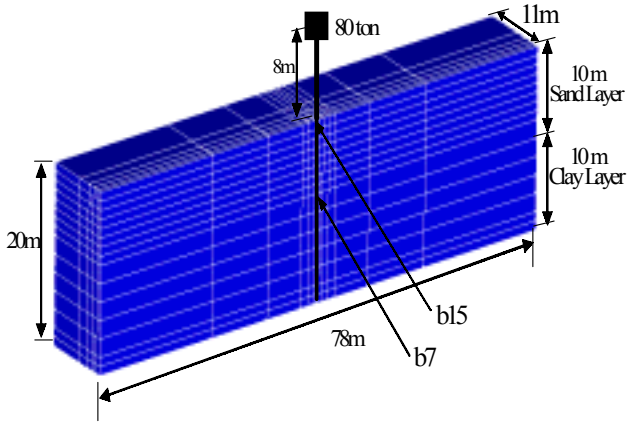

Fig. 3. Finite element mesh

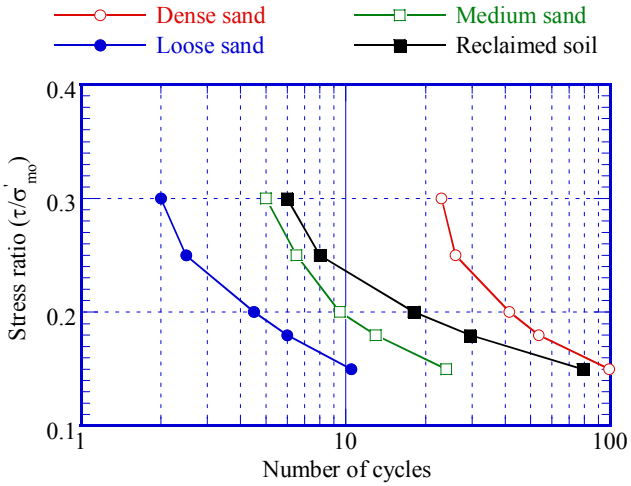

Fig 4. Liquefaction strength curves of different sandy soils

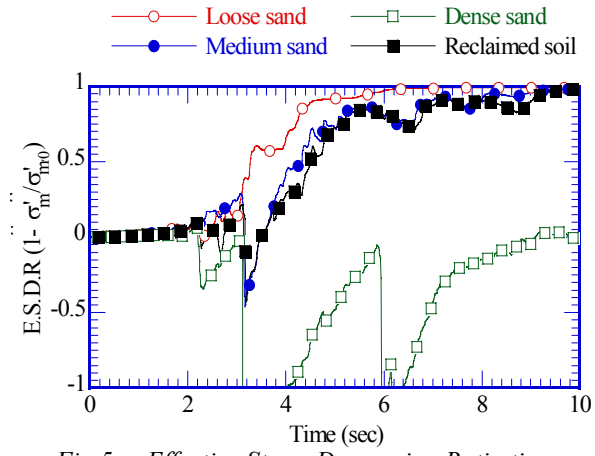

Fig.5. Effective Stress Decreasing Ratio time profile

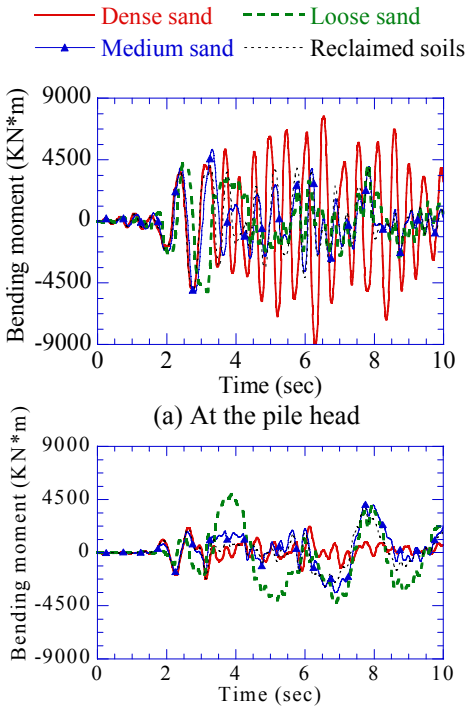

(a) At the pile head

(b) At the segment at the boundary

Fig.6. Bending moment time profile

Figure 7 shows the distribution of bending moment when the maximum bending moment takes place in each case and Figure 8 shows the distribution of bending moment at the end of the seismic event.

They show the although maximum bending moment takes place at pile head (b15) in every case, the development of the bending moment in the ground varies due to the features of soil.

The large bending moment takes place in lower pile segment (b7) in the cases of liquefiable soils but at upper pile segment (b15) in the case of dense sand at the end of the seismic event.

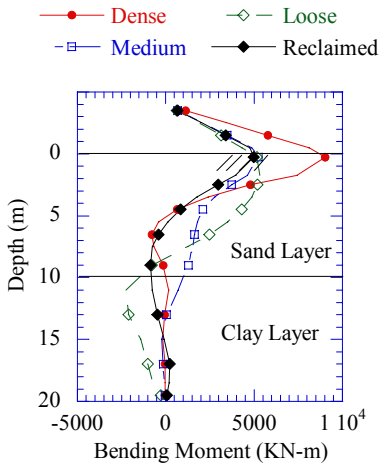

Fig.7. Distribution of bending moment

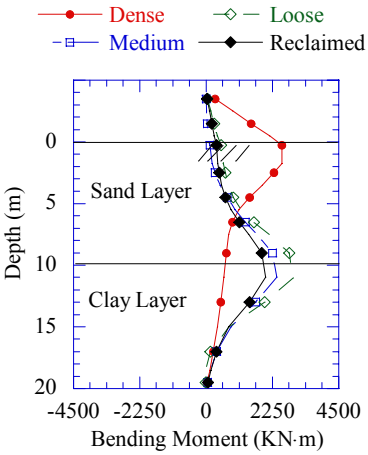

Fig.8. Distribution of bending Moment at the end of the event

CONCLUSIONS

The following conclusions are obtained from the present study:

(a) The maximum bending moment at pile head in non-liquefied ground is larger than those in liquefiable ground; (b) liquefaction process may greatly increase the

bending moment and shear force of the pile at the boundary between two different layers; (c) the responses in the cases of medium dense sand and reclaimed soils are similar to the case of dense sand at the beginning; and (d) after the effective stress decreases significantly in the cases of medium dense sand and reclaimed soils, the response becomes similarly to that of loose sand.

REFERENCES

Biot, M.A. [1962], "Mechanics of Deformation and Acoustic Propagation in Porous Media", *J. Applied Physics*, Vol. 33, No. 4, pp.1482-1498.

Lu, C.W., Oka, F., Zhang, F., and Yashima, A. [2002], "Mechanical behavior of single and group piles before and after liquefaction", *Proc. of 1st International Workshop on New Frontiers in Computational Geotechnics*, Calgary.

Oka, F., Yashima, A., Tateishi, A., Taguchi, Y. and Yamashita, S. [1999], "A cyclic elasto-plastic constitutive model for sand considering a plastic-strain dependence of the shear modulus", *Geotechnique*, Vol.49, No.5, pp.661-680.

Oka. F. [1992], "A cyclic elasto-viscoplastic constitutive model for clay based on the non-linear-hardening rule", *Proc. 4th int. Sym. on Numerical Models in Geomechanics*, Swansea, pp. 105-114.

Zhang, F. and Kimura, M. [2002], "Numerical prediction of the dynamic behaviors of an RC group-pile foundation", *Soils and Foundations*, Vol. 42, No. 3, pp. 77-92.

Zienkiewicz, O.C. and Bettes, P.[1982], "Soils and Other Saturated Media under Transient, Dynamic Conditions, General Formula and Validity of Various Simplifying Assumptions", *Soil Mechanics-Transient and Cyclic Loads*. New York: John Wiley & Sons, pp.1-16.

Table 2 Material Parameters for Pile

Young's Modulus of concrete E_c (kN/m^2)	2.5E7
Diameter of pile D (m)	1.5
Compressive strength of concrete f_c (kN/m^2)	36000.00
Tensile strength of concrete f_t (kN/m^2)	3000.00
Degrading parameter of concrete β_c	0.20690
Young's Modulus of steel E (kN/m^2)	2.1E8
Diameter of reinforcement d (m)	0.029
Number of reinforcement N	24
Yielding strength of steel Y_s (kN/m^2)	3.8E5

Table 1 Material parameters for Soils

	Dense Sand	**Medium Dense Sand**	**Loose Sand**	**Reclaimed Soil**	**Soft Clay**
Density ρ (t/m^3)	2.0	2.0	2.0	2.0	1.7
Void Ratio e_0	0.6	0.8	0.8	0.420	1.4
Coefficient of permeability k (m/s)	1.5×10^{-5}	3.0×10^{-5}	3.0×10^{-5}	2.0×10^{-4}	1.0×10^{-9}
Compression Index λ	0.020	0.03	0.03	0.01	0.100
Swelling index κ	0.002	0.002	0.003	0.001	0.020
Stress Ratio of Failure State M^*_f	1.10	1.00	0.80	1.19	1.31
Stress Ratio at Maximum Compression M^*_m	0.85	0.80	0.70	0.91	1.28
Normalized Shear Modulus G_0/σ'_{m0}	1980.0	1060.0	500.0	2140.0	300.0
Hardening Parameter B_0^*, B_1^*, C_f *for sand* B_0^*, B_s^*, B_t^* *for clay*	8500, 85, 0	4000, 400, 0	2500, 25, 0	5500, 55, 0	500, 50, 0
Shear Wave Velocity V_s (m/s)	180 (σ'_0=102 KN/m^2)	134 (σ'_0=102 KN/m^2)	92 (σ'_0=102 KN/m^2)	190 (σ'_0=102 KN/m^2)	127 (σ'_0=138 KN/m^2)
Sand					
Control parameter of anisotropy C_d	2000	2000	2000	2000	-
Parameter of Dilatancy D_0, n	1.0, 2.5	1.0, 2.0	1.0, 1.0	1.0, 4.0	-
Reference Value of Plastic Strain γ^P_r	0.008	0.003	0.001	0.002	-
Reference Value of Elastic Strain γ^E_r	0.09	0.035	0.005	0.01	-
Clay					
Viscoplastic Parameter C_{01} (1/s)	-	-	-	-	5.5×10^{-6}
Viscoplastic Parameter C_{02} (1/s)	-	-	-	-	7.8×10^{-7}
Viscoplastic Parameter m_0'	-	-	-	-	14